



Metallicity dependence of light and heavy s-process elements in AGB stars

R. Gallino^{1,2}, S. Bisterzo^{1,3}, O. Straniero⁴, I.I. Ivans^{5,6}, and F. Käppeler³

¹ Dipartimento di Fisica Generale, Università di Torino, via P. Giuria 1, 10025 Torino, Italy

² Centre for Stellar and Planetary Astrophysics, School of Mathematical Sciences, Building 28, Monash University, 3800 Victoria, Australia

³ Forschungszentrum Karlsruhe, Institut für Kernphysik, D-76021 Karlsruhe, Germany

⁴ Osservatorio Astronomico di Collurania, INAF, Teramo, 64100, Italy

⁵ The Observatories of the Carnegie Institution of Washington, Pasadena, CA, USA

⁶ Princeton University Observatory, Princeton, NJ, USA
e-mail: gallino@ph.unito.it

Abstract. The s-process in AGB stars is far from being a unique process. Observations of s-enriched stars indicate that a multiplicity of neutron exposures are needed at each metallicity. Model predictions of AGB stars of different metallicity, initial mass, and different ¹³C-pocket efficiencies, are presented and discussed, pointing out in particular their ability to reproduce the range of observed s-process elemental distributions in very metal-poor C-rich and s-rich objects.

Key words. Stars: C and s rich – Stars: abundances – Stars: Population II – Stars: nucleosynthesis

1. Introduction

Three s-process components were anticipated by the classical analysis (Clayton and Rassbach 1967; Käppeler et al. 1982): the weak, the main, and the strong s-component. The s-process is characterized by a generally smooth curve $\sigma(A)N_s(A)$ versus atomic mass number A, interrupted by steep decreases in correspondence of the magic neutron numbers $N = 50, 82$ or 126 , where the neutron capture cross sections are very small and the resulting s-process abundances are large. The main component and the strong component are synthesized by low mass stars ($1.3 \leq M/M_\odot \leq$

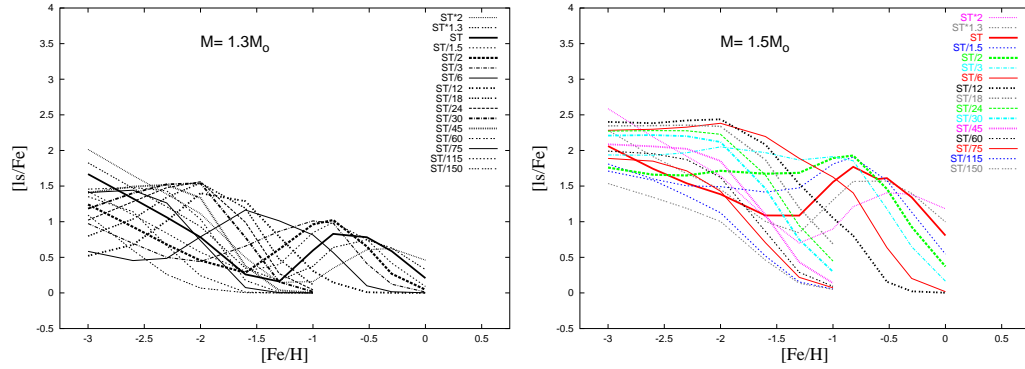
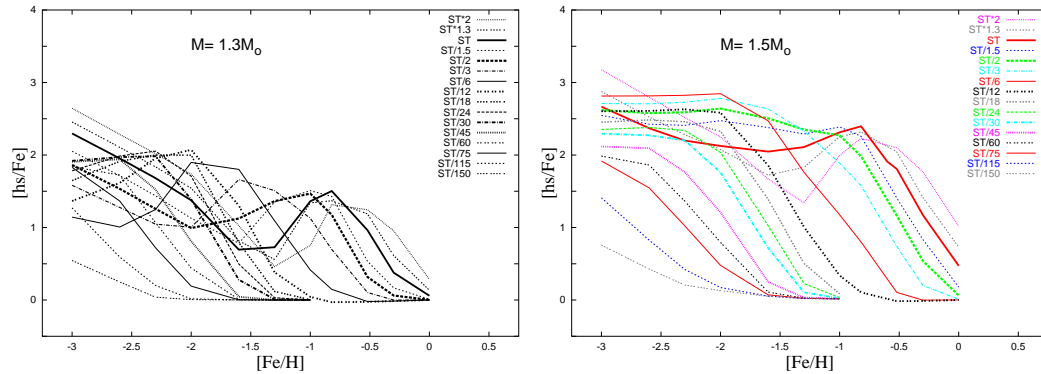
4), while climbing the Asymptotic Red Giant Branch (AGB) and progressively losing their envelope by efficient stellar winds. During the AGB phase, the star suffers a series of alternate burning in the H-shell and in the He shell. A recurrent He shell flash, called thermal pulse, makes the whole He-rich zone (He intershell) convective for a short period of time.

Partial burning of He in the thermal pulse enriches the He intershell with ¹²C (of mass fraction $X(^{12}\text{C}) \approx 0.25$). At the quenching of a thermal instability, the bottom of the convective envelope penetrates in the top region of the He intershell, mixing freshly nucleosynthesized ¹²C and s-process elements with the envelope (third dredge up event). During the

Send offprint requests to: R. Gallino

Table 1. [La/Eu] expectations in AGB stars of mass $M = 1.3 M_{\odot}$ and $[\text{Fe}/\text{H}] = -2.6$.

[La/Eu]	nr	rp0p5	rp1	rp1p5	rp2
ST	0.88	0.82	0.66	0.37	-0.04
ST/12	0.80	0.69	0.45	0.08	-0.35
ST/75	1.06	0.82	0.46	0.02	-0.46

**Fig. 1.** Predicted [ls/Fe] versus metallicity for different ^{13}C -pocket efficiencies. The two plots correspond to model of $M = 1.3 M_{\odot}$ (Left panel) $M = 1.5 M_{\odot}$ (Right panel).**Fig. 2.** Predicted [hs/Fe] versus metallicity for different ^{13}C -pocket efficiencies. The two plots correspond to model of $M = 1.3 M_{\odot}$ (Left panel) and $M = 1.5 M_{\odot}$ (Right panel).

third dredge up, the H-rich envelope and the He intershell come into contact, favoring the penetration of a small amount of protons in the top layers of the He intershell. The discontinuity in the chemical composition makes the contact region unbalanced against the criterion of convective neutrality (see Straniero et al. 2006; Cristallo et al., These Proceedings). The phenomenon is difficult to be treated, and

up to now the resulting amount of protons that are diffused and its profile in mass have been treated parametrically within a range of possibilities (Gallino et al. 1998; Busso, Gallino and Wasserburg 1999). Once this zone is reheated, proton capture on the abundant ^{12}C gives rise to the formation of a so-called ^{13}C -pocket, which provides the major source of neutrons in AGB stars. Indeed, later on the

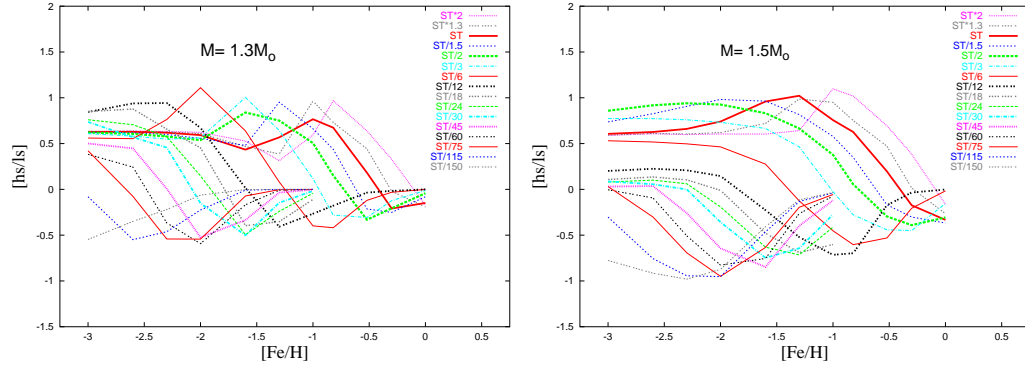


Fig. 3. Predicted [hs/ls] versus metallicity for different ^{13}C -pocket efficiencies. The two plots correspond to model of $M = 1.3 M_{\odot}$ (Left panel) and $M = 1.5 M_{\odot}$ (Right panel).

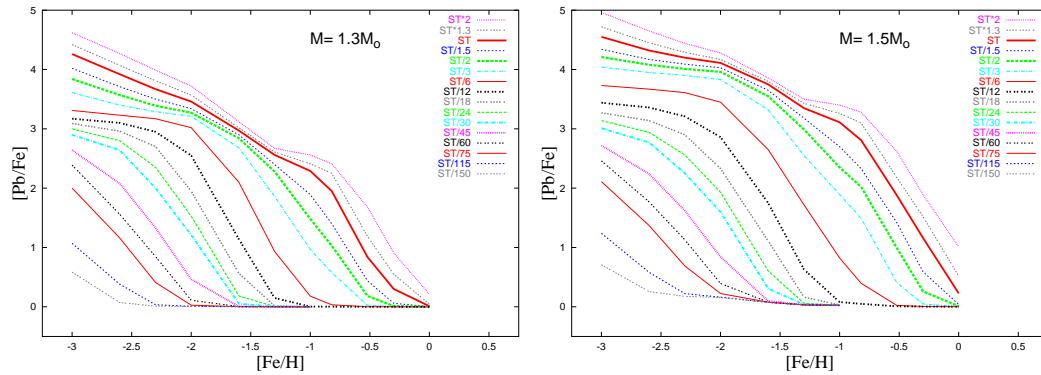


Fig. 4. The first intrinsic indicator [Pb/hs] versus metallicity for AGB stars with different ^{13}C -pocket efficiencies. The two plots correspond to model of $M = 1.3 M_{\odot}$ (Left panel) and $M = 1.5 M_{\odot}$ (Right panel).

$^{13}\text{C}(\alpha,n)^{16}\text{O}$ reaction takes place in radiative conditions before the development of the next thermal instability, boosting the s process. A second, marginal, neutron burst occurs during the thermal pulse, driven by the marginal occurrence of the $^{22}\text{Ne}(\alpha,n)^{25}\text{Mg}$ reaction. It provides a small neutron exposure, but with a high peak neutron density, modifying the final s-process composition at branchings along the s-path that are sensitive to the neutron density or to the temperature. The s-component is far from being a unique process, depending on the efficiency of the so-called ^{13}C -pocket, the initial mass, and the metallicity. Comparison of AGB stellar model calculations at various metallicities with spectroscopic observations of different stellar populations clearly demon-

strates the vast multiplicity of s-process components. One of the major evidences is provided by low-metallicity C-rich and s-process rich stars (the *lead stars*).

2. AGB stars and s-process predictions

For a given ^{13}C pocket efficiency, decreasing the metallicity and starting from a solar composition, the s-process fluence progressively feeds the first s-peak elements Sr, Y, Zr (*light - s*, ls) then the second s-peak at Ba, La, Ce, Pr, Nd (*heavy - s*, hs) and eventually the third s-peak at the termination point of the s-process (Pb). The solar system main component is apparently best reproduced by an AGB model of

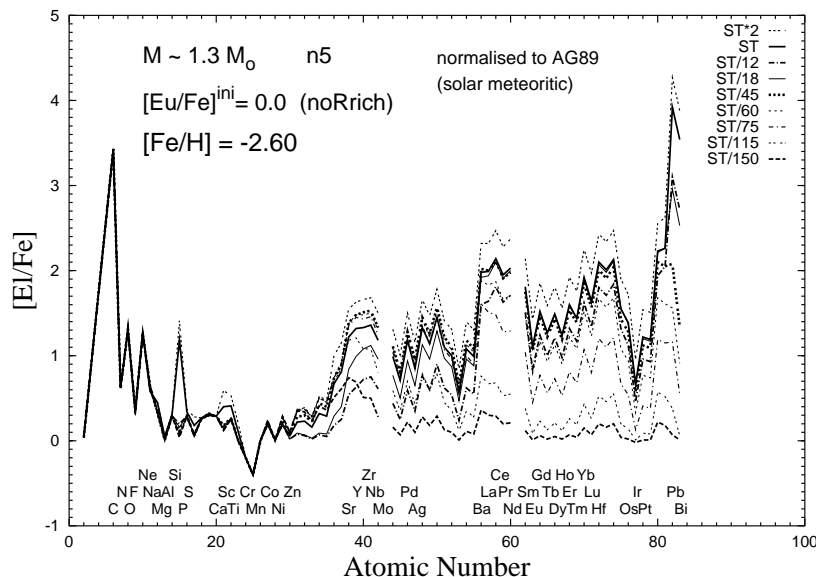


Fig. 5. Elemental composition in the envelope at the last third dredge up episode for an AGB model of initial mass $M = 1.3 M_{\odot}$, $[\text{Fe}/\text{H}] = -2.6$ and for different ^{13}C -pocket efficiencies (solar-scaled initial r-process distribution).

half-solar metallicity while adopting the ^{13}C -pocket of Gallino et al. (1998, Case ST). It should however be clear that the solar system s-process distribution is the result of all previous generations AGB stars in the Galaxy. For a given metallicity, varying the ^{13}C pocket efficiency a large spread of $[\text{Pb}/\text{hs}]$, by two orders of magnitude, is predicted, in agreement with spectroscopic observations. In particular, the strong s-component in the solar system is the result of all previous generations AGB stars in the Galactic Halo, feeding 50% of solar ^{208}Pb and 20% of solar Bi (Travaglio et al. 2001).

In Fig. 1 we show our AGB model predictions of $[\text{ls}/\text{Fe}]$ for stars of initial mass $1.3 M_{\odot}$ (left panel) and $1.5 M_{\odot}$ (right panel) versus $[\text{Fe}/\text{H}]$ for a large range of ^{13}C pocket efficiencies. The AGB models of $1.3 M_{\odot}$ suffer a limited number of third dredge up episodes with also less amount of He intershell mass mixed per episode with the envelope. Thus, for given metallicity and ^{13}C pocket choice, a lower $[\text{ls}/\text{Fe}]$ results that in the case of AGB star of mass 1.5 to $3 M_{\odot}$. Note that very similar distributions are obtained in AGB stars of initial mass 1.5 and $2 M_{\odot}$. Accounting for dif-

ferent choices of the ^{13}C pocket and for different initial masses, a large spread of $[\text{ls}/\text{Fe}]$ is predicted at any metallicity, covering more than two orders of magnitude. Fig. 2 shows the corresponding AGB model predictions for $[\text{hs}/\text{Fe}]$. In Fig. 3 we report the intrinsic indicator $[\text{hs}/\text{ls}]$, which is a measure of the mean neutron exposure, that is a signature of the relative s-process distribution between the heavy and the light s-elements. A large spread at any given metallicity is predicted also for $[\text{hs}/\text{ls}]$ from a maximum expectation close to 1 dex and a minimum value that reaches -1 . As recalled in the Introduction, for $[\text{Fe}/\text{H}] = -0.3$ the ST case best reproduces the main component in the solar system, at $[\text{hs}/\text{ls}] = -0.2$. It is clear from Fig. 3 that about the same distribution at various metallicities may be obtained with a proper choice of the ^{13}C pocket. Given that neutrons are released by the primary source ^{13}C (made in the pocket from proton capture on primary ^{12}C), while the main neutron seed for the build-up of the s-elements, ^{56}Fe scales with the metallicity, the number of neutrons captured by Fe seed grossly scales

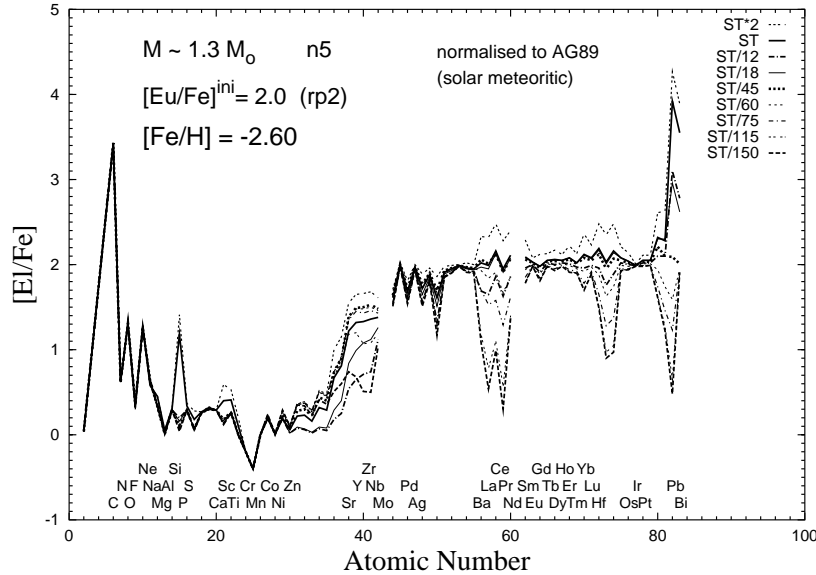


Fig. 6. Elemental composition in the envelope at the last third dredge up episode for an AGB model of initial mass $M = 1.3 M_{\odot}$, $[\text{Fe}/\text{H}] = -2.6$ and for different ^{13}C -pocket efficiencies (The same as Fig. 5 but with an extreme initial r-process enhancement normalized to $[\text{Eu}/\text{Fe}]^{\text{ini}} = 2$).

as $^{13}\text{C}/^{56}\text{Fe}$. For a given choice of the ^{13}C pocket efficiency and decreasing the metallicity, a maximum of $[\text{hs}/\text{ls}] \approx 1$ is reached, but then it further decreases, since the neutron fluence overcomes the ls and the hs peaks and directly feeds ^{208}Pb at the termination point of the s-process. Consequently, AGB stars at halo metallicities mostly produce Pb. This is shown in Fig. 4, where the predicted $[\text{Pb}/\text{Fe}]$ by AGB models of 1.3 and $1.5 M_{\odot}$ is reported versus $[\text{Fe}/\text{H}]$. This implies that for halo stars, besides $[\text{hs}/\text{ls}]$, a second intrinsic indicator is needed to fully characterize the elemental distribution of the s-process. The comparison of predicted $[\text{Pb}/\text{hs}]$ in low metallicity AGB stars with observational evidences of a couple of dozen C-rich and s-process-rich stars observed in the last few years is presented and discussed in Bisterzo et al. (These Proceedings). Note that the halo stars presently observed are all binary AGB stars (extrinsic AGB), where the more massive AGB transferred part of its C-rich and s-rich envelope by efficient stellar winds on the less massive companion (now observed), leaving its degenerate CO core as a white dwarf. In fact, the typi-

cal mass of Halo stars at the turnoff is $0.8 - 0.9 M_{\odot}$, and their envelope mass is too small for the third dredge up phenomenon to occur (see Straniero et al. 2006). Note that according to Lucatello et al. (2005) all C-rich and s-rich metal-poor stars show binarity from their radial velocity temporal variations. In Fig. 5 we present the resulting elemental composition in the envelope of an AGB model of initial mass $M = 1.3 M_{\odot}$, for a metallicity $[\text{Fe}/\text{H}] = -2.6$ and for a range of ^{13}C pocket efficiencies. A very high abundance of ^{12}C in the envelope results from these models. However, a substantial fraction of ^{12}C may be converted to primary ^{14}N by the the operation of a slow mixing in the bottom layer of the envelope (the so-called *Cool Bottom Process*, CBP, see the review of Wasserburg, Busso, Gallino and Nollett 2006). Among the very metal-poor stars C-rich and s-process rich a consistent number of objects show the unusual characteristic of being also r-process rich (Ivans et al. 2005; and These Proceedings). Vanhala and Cameron (1998) showed through numerical simulations how the supernova ejecta may

interact with a nearby molecular cloud, polluting it with fresh nucleosynthesized material and likely triggering the formation of binary system consisting of stars of low mass. A major indicator of the s+r enrichment in these stars is provided by the [La/Eu] ratio, as reported in Table 1, where the pre r-enrichment ranges from *nr* (no enrichment) to *rp2* corresponding to $[\text{Eu}/\text{Fe}]^{\text{ini}}=2$. Lanthanum is a major s-process element, whose solar abundance is contributed by 70% by the s-process (Winckler et al. 2006). Europium is mostly made by the r-process (94,2% of its solar abundance). In Fig. 6 the elemental composition in the envelope of an AGB model of initial mass $M = 1.3 M_{\odot}$ is shown for the same metallicity and range of ^{13}C pocket efficiencies of Fig. 5, but under the assumption of an extreme pre r-enrichment in the parental cloud, normalized to $[\text{Eu}/\text{Fe}]^{\text{ini}} = 2.0$ (*rp2*). The choice of the initial r-rich isotope abundances fractions normalized to Eu is based on the residuals $r = 1 - s$ calculated by Arlandini et al. (1999).

Acknowledgements. MURST-FIRB project "Astrophysical Origin of the Heavy Elements beyond Iron". Thanks to the Aspen Center for Physics for insightful discussions relating to this work during the "Summer School on the s-process" organised by R. Reifarth and F. Herwig.

References

- Arlandini, C. et al. 1999, *ApJ*, 525, 886
 Busso, M., Gallino, R. & Wasserburg, G. J. 1999, *ARA&A*, 37, 239
 Clayton, D. D., Rassbach, M. 1967, *ApJ*, 148, 69
 Gallino, R. et al. 1998, *ApJ*, 497, 338
 Ivans, I.I., et al. 2005, *ApJ*, 627, 145
 Lucatello, S. et al. 2005, *ApJ*, 625, 825
 Käppeler, F. et al. 1982, *ApJ*, 257, 821
 Straniero, O., Gallino, R. & Cristallo, S., in Nuclear Astrophysics (eds. K. Langanke, F.-K. Thielemann and M. Wiescher), Special Issue of *Nucl. Phys. A.*, in press,
 Travaglio, C., Gallino, R., Busso, M., Gratton, R. 2001, *ApJ*, 549, 346
 Vanhala, H. A. T. & Cameron, A. G. W. 1998, *ApJ*, 508, 291
 Wasserburg, G. J., Busso, M., Gallino, R., Nollett, K. M., in Nuclear Astrophysics (eds. K. Langanke, F.-K. Thielemann and M. Wiescher), Special Issue of *Nucl. Phys. A.*, in press (astro-ph/0602551)
 N. Winckler, N., et al. & Pignatari, M. 2006, *ApJ*, in press